Colloids and Surfaces B: Biointerfaces 93 (2012) 188–194

Contents lists available at SciVerse ScienceDirect

Colloids and Surfaces B: Biointerfaces

journal homepage: www.elsevier.com/locate/colsurfb

# Facile construction of functional biosurface via SI-ATRP and "click glycosylation"

Wantong Song[a,b], Chunsheng Xiao[a,b], Liguo Cui[a], Zhaohui Tang[a], Xiuli Zhuang[a], Xuesi Chen[a,*]

[a] Key Laboratory of Polymer Ecomaterials, Changchun Institute of Applied Chemistry, Chinese Academy of Sciences, Changchun 130022, PR China
[b] Graduate University of Chinese Academy of Sciences, Beijing 100039, PR China

ARTICLE INFO

*Article history:*
Received 16 August 2011
Received in revised form 3 January 2012
Accepted 3 January 2012
Available online 11 January 2012

*Keywords:*
Biosurface
Glycosylation
SI-ATRP
Click chemistry

ABSTRACT

Construction of high density glycosylated surfaces is important in the investigation of interactions between pathogens and surface carbohydrates. In this work, we provided a flexible method for glycosyl surface fabrication by combination of surface-initiated atom transfer radical polymerization (SI-ATRP) and copper-catalyzed azide-alkyne 1,3-dipolar cycloaddition (CuAAC) reaction. Through this strategy, we got a very high surface glycosyl density of about 4 nmol/cm$^2$ with the surface "click" efficiency of nearly 50%. Then the carbohydrate decorated surfaces were used to mimic cell surfaces and specific recognition of mannose with *Escherichia coli* was observed. We believe the methodology provided here can be used as a facile way for construction of a wide range of functional biosurfaces.



## 1. Introduction

Cell surface saccharides play important roles in numerous biological phenomena [1,2]. To better understand the mechanisms that lead to carbohydrate-mediated pathogen infections, it is important to study bacterial adhesion to tailored interfaces and to determine the carbohydrate binding fingerprints [3]. In addition, high surface carbohydrate density is a prerequisite for mimicking the multivalent interaction, or "glycoside cluster effect" [4].

Great interests and advances in the field of glycomics [5–8] have accelerated the development of surface saccharide presenting platform [9–11]. Carbohydrate microarrays and biosensors have been fabricated by physical self-assemble [12] or covalent immobilization [13–15] of sugars directly onto functionalized solid surfaces. Synthetic glycopolymer modified surfaces provide another simplified model of the clustered carbohydrates presented on the membrane of eukaryotic cells. Such model surfaces present the specific ligands in a non-interactive ("non-fouling") background and provide means for adjusting the surface ligand density [16].

Since ease of preparation and versatility are quite important factors in chip fabrication, two-step strategy, which shows more choice and flexibility, has gained more and more attention [17–19]. In this strategy, surfaces are firstly covered with polymer layers, and functional pendants are linked to the created coatings subsequently. However, accurate control and effective reaction are two critical determinants for accessibility and reproducibility of the functional surfaces.

SI-ATRP is an interesting and powerful method for surface modification [20,21]. It has got much attention in developing biofunctional coatings [22]. Polymer brushes covered chips prepared from SI-ATRP provide high binding capacity and show much more potential compared with 2D planar [23]. Also, in contrast to spin-coated polymer films or brushes obtained from "graft to" method, SI-ATRP provides relative high chain densities and accurate control over brush thickness, composition, and architecture [20]. This has long been recognized since glycopolymer brushes were prepared using surface-initiated polymerization of protected [24] or unprotected [25] glucose-containing monomers, and as were achieved on various substrates [18]. The concept of "click" chemistry proposed by Sharpless and co-workers pertains to reactions that are easily to perform, high yielding, and tolerant of oxygen and water [26]. The CuAAC reaction, a widely utilized "click" reaction, was extensively used for surface functionalization and exhibited very high efficiency [15,23].

Herein, a facile method for construction of biosurface with high glycosyl density is reported. Silicon surface was firstly covered with polymer brushes containing "clickable" alkyne pendants prepared by SI-ATRP, and then microwave assisted CuAAC reaction [27] was adopted for immobilizing azido biomolecules onto the brushes. The surface modification process was well-characterized by contact angle, ellipsometry, XPS and AFM, and the surface glycosyl densities were estimated based on XPS quantitative analysis. Finally, recognition and adsorption of *Escherichia coli* and mannose decorated surfaces were also studied.

* Corresponding author. Tel.: +86 431 85262112; fax: +86 431 85262112.
*E-mail address:* xschen@ciac.jl.cn (X. Chen).

0927-7765/$ – see front matter © 2012 Elsevier B.V. All rights reserved.
doi:10.1016/j.colsurfb.2012.01.002

## 2. Materials and methods

### 2.1. Materials

D-(β)-Galactose (98%), and D-(β)-mannose (98%), bromoisobutyryl bromide (BIBB, 98%) were purchased from Alfa Aesar and used as received. Boron trifluoride diethyl ether and methacryloyl chloride (97%) were purchased from Aladdin. Propargyl alcohol (Zhejiang Realsun Chemical Industry Co. Ltd., China, 99%) was used as obtained.

The inhibitor in oligo (ethylene glycol) methacrylate (OEGMA, Aldrich, $M_n$ = 454) was removed by passing through a basic aluminum oxide column, and 1,1,4,7,7-pentamethyldiethylenetriamine (PMDETA, Aldrich, 99%) was freed from its inhibitor (phenothiazine) via distillation under reduced pressure. SI-ATRP was performed on silicon wafers (100-oriented, polished on one side) which were cut into pieces of 1 cm × 1 cm. Copper (I) bromide (CuBr, Sinopharm, 98%) was purified by being stirred in acetic acid, washed with methanol, and then dried under vacuum. 10-Undecenol (Alfa Aesar, 98%) was distilled out under reduced pressure and stored in the dark.

2-Propynyl methacrylate (PPMA) was synthesized according to published protocols [29,30]. 2-Azidoethanol was prepared from 2-bromoethanol and sodium azide in the presence of sodium hydroxide. All other reagents and solvents were purchased from Sinopharm Chemical Reagent Co. Ltd., China and used as received unless stated.

### 2.2. Synthesis of azido-monomers

*3-Azido-7-hydroxycoumarin* (**1**, Scheme 1).

Prepared as described by Sivakumar et al. [28], 46% overall yield.

IR: $\nu$ = 3296, 2125, 1680, 1620, 1321 $cm^{-1}$. $^1H$ NMR (400 MHz, DMSO) $\delta$ = 6.74 (d, 1H), 6.79 (d, 1H), 7.47 (d, 1H), 7.56 (*s*, 1H) ppm.

*Azido-(tri) ethylene glycol* (**2**, Scheme 1).

Prepared as described by Mei et al. [29], with a yield of 88%.

IR: $\nu$ = 2875, 2107, 1453, 1302, 1111 $cm^{-1}$. $^1H$ NMR (400 MHz, $CDCl_3$) $\delta$ = 3.24 (*s*, 3H, C***H***$_3$O), 3.39 (*m*, 2H, C***H***$_2$N$_3$), 3.52 (*m*, 2H, C***H***$_2$CH$_2$N$_3$), 3.60 (*m*, 8H, C***H***$_2$O) ppm.

*2′-Azidoethyl-O-a-D-mannopyranoside* (**3**, Scheme 1) and *2′-azidoethyl-O-b-D-galactopyranoside* (**4**, Scheme 1)

The two azido-monosaccharides were prepared similarly as that described by Geng et al. [30]. Briefly, D-mannose (D-galactose) was firstly protected by acetic anhydride, and then the 2-hydroxyl was substituted by azidoethanol. Finally, the protected acetic groups were removed by sodium methoxide in methanol. The final product was purified by flash column chromatography and white solid was obtained.

For 2′-azidoethyl-O-a-D-mannopyranoside, 12% overall yield. IR: $\nu$ = 3358, 2927, 2097, 1644, 1301, 1262, 1132, 1056 $cm^{-1}$. $^1H$ NMR (400 MHz, $D_2O$): $\delta$ = 3.45 (*m*, 2H, C***H***$_2$N$_3$), 3.55–3.60 (*m*, 2H, C***H***$_2$CH$_2$N$_3$), 3.61–3.67 (*m*, 2H, C***H***$_2$OH), 3.67–3.91 (*m*, 4H, C***H***), 4.92 (*d*, 1H, C***H***) ppm.

For 2′-azidoethyl-O-b-D-galactopyranoside, 12% overall yield. IR: $\nu$ = 3322, 2953, 2098, 1644, 1303, 1265, 1121, 1061 $cm^{-1}$. $^1H$ NMR (400 MHz, $D_2O$), $\delta$ = 3.57 (*m*, 2H, C***H***$_2$N3), 3.60 (*m*, 1H, C***H***), 3.64–3.72 (*m*, 2H, C***H***$_2$CH$_2$N$_3$), 3.76–3.80 (*m*, 2H, C***H***$_2$OH), 3.83 (*m*, 1H, C***H***), 3.93 (*m*, 1H, C***H***), 4.05 (*m*, 1H, C***H***), 4.46 (*d*, 1H, C***H***) ppm.

### 2.3. Preparation of POEGMA/PPMA-grafted silicon wafers

#### 2.3.1. Substrate preparation

Single-side polished, silicon (1 0 0) wafers were cut into pieces of 1 cm × 1 cm and cleaned with "Piranha" solution (concentrated $H_2SO_4$/30% $H_2O_2$ = 7:3, v/v) for 2 h at 80 °C. The freshly cleaned sample was immersed in argon-saturated, 2% HF solution for 15 s followed by rapid rinse with argon-saturated Millipore water and dried with a stream of argon.

The freshly prepared Si (100)-H substrate was placed inside a 10 mL quartz tube and degassed for 10 min under vacuum. Then 5 mL 20% undecenol in hexane was injected. The hydrosilylation was performed under 254 nm UV illumination with a handheld illuminator (ZF-20D, Gongyi Yuhua Co. Ltd. power of 8 W) for 5 h. The sample was washed thoroughly with absolute ethanol and water followed by drying under a stream of argon.

#### 2.3.2. Immobilization of initiator layer

The hydroxyl-functionalized surface was incubated in 10 mL of dry dichloromethane containing 1 mL BIBB. The reaction was carried out at room temperature for 12 h. The initiator-immobilized silicon wafers were cleaned with dichloromethane, acetone and water, and dried under argon flow.

#### 2.3.3. Surface-initiated ATRP of OEGMA/PPMA

ATRP grafting of OEGMA and PPMA from initiator-functionalized silicon wafers was carried out using the freeze-pump-thaw method. OEGMA (1.35 g, 3 mmol), PPMA (0.25 g, 2 mmol), PMDETA (8.7 mg, 0.05 mmol) and CuBr (7.2 mg, 0.05 mmol) were dissolved in a 4:1 mixture of methanol and water (10 mL). The reaction solution was degassed through three

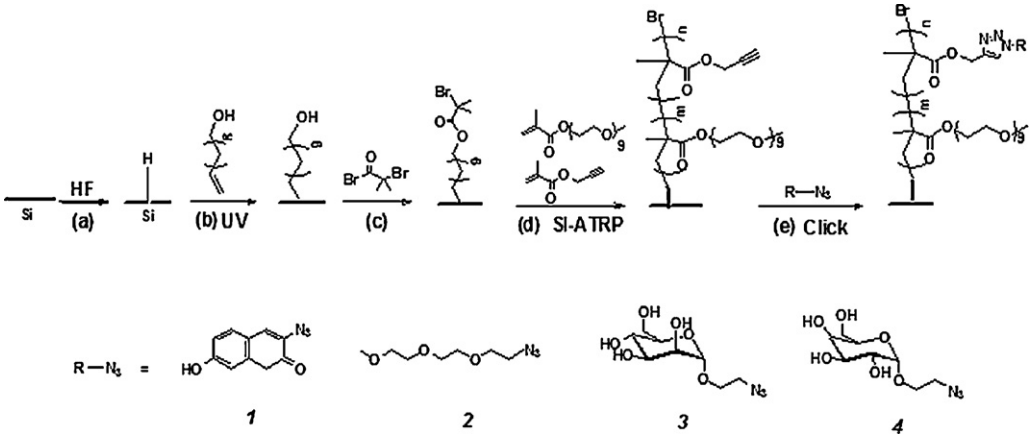


**Scheme 1.** Process for preparation of functionalized surface. (a) Silicon surface was treated with dilute HF to afford a Si—H surface; (b) photoactivated hydrosilylation of Si—H and undecenol; (c) after reaction with BiBB, initiator layer was formed with Br decorated on surfaces; (d) Si-ATRP of OEGMA and PPMA (3:2 in ratio, 12 h); (e) Azido molecules "click" onto the alkyne pendants (***1***, ***2***, ***3***, ***4*** are coumarin, (tri) ethylene glycol, mannose and galactose respectively) under microwave conditions.

**Table 1**
Characterization of modified surfaces and graft density calculation.

| | Contact angle (°)[a] | Dry thickness (Å)[b] | *N* (%)[c] | *N* (%)[d] | "Click" efficiency (%) | Graft density (nmol/cm$^2$) |
|---|---|---|---|---|---|---|
| Si–Br | 84.5 ± 1.1 | 46.1 ± 2.3 | | | | |
| Si–ATRP | 58.8 ± 0.5 | 268.0 ± 9.1 | | | | |
| Si–$EG_3$ | 45.2 ± 1.4 | 281.4 ± 7.2 | 3.8 | 4.4 | 86 | 6.7 |
| Si–Gal | 37.2 ± 1.1 | 273.0 ± 10.5 | 2.5 | 4.1 | 61 | 4.7 |
| Si–Man | 35.5 ± 0.8 | 271.9 ± 8.1 | 2.0 | 4.1 | 49 | 3.8 |

(a) The contact angles are measured at 25 °C, each value was averaged from five parallel measurements. (b) The dry thickness were measured by ellipsometry, represent an average over three data points taken from the same substrate at different points. (c) Results from XPS quantitative analysis; (d) Results calculated according to Eq. (1). The "click" efficiency is the ratio of (c) over (d). Graft densities are calculated according to Eq. (4).

freeze–pump–thaw cycles before being added separately to glass vessels in which the initiator functionalized wafers were placed.

The polymerization was carried out at 40 °C for 12 h. After reaction, the Si-*g*-copolymer hybrid was washed thoroughly by extraction with copious amounts of ethanol and doubly distilled water. The hybrid was subsequently immersed in a large volume of water for about 12 h to ensure the complete removal of the reactants.

#### 2.3.4. Surface CuAAC reactions

The surface CuAAC reaction was performed using a microwave assistant condition. Silicon substrates coated with polymer brushes were placed in deionized water/ethanol solution (20 mL, 3:7, v/v), then 0.04 mmol of the preferred azido molecule (***1***, ***2***, ***3***, ***4***, Scheme 1) was added (for ***1***, the solvent was DI water/ethanol/DMF = 5:2:3 to ensure the solubility). The solution was bubbled with argon for 20 min, then sodium L-ascorbate (40 mg), CuBr (10 mg), and PMDETA (10 mg) were added. After sealed, the vessel was placed in a microwave reactor (Beijing Xianghu Co. Ltd.) set at 500 W at 50 °C for 30 min. After reaction, the substrate was thoroughly washed with deionized water, acetone, ethanol, (for ***1***, DMF was used), and then dried in a stream of argon.

### 2.4. Surface characterization

The chemical composition of the modified silicon surfaces was determined by X-ray photoelectron spectroscopy (XPS). XPS measurements were performed with Thermo ESCALAB 250 (Thermo Electron Corporation, U.K.) at room temperature by using an Al Kα X-ray source ($h\nu$ = 1486.6 eV). The main chamber of the XPS instrument was maintained at $10^{-9}$ Torr. Pass energies of 50 and 20 eV were used to obtain the survey scan spectra and high-resolution spectra, respectively.

The static water contact angles of the pristine and functionalized silicon surfaces were measured using the sessile drop method with a 2 μL water droplet, in a KRÜSSDSA10-MK2 contact angle measuring system (Krüss, Germany) at ambient temperature.

The thickness of the polymer brushes grafted on the silicon substrate was determined by a variable angle spectroscopic ellipsometer (Model VASE, J.A. Woollam Inc., Lincoln, NE), at an angle of incidence of 70°. The calculation method was based on a two-layer silicon/polymer brush model, assuming the polymer brushes to be isotropic and homogeneous and Cauchy model was used for simulation. All reported ellipsometric thicknesses represent an average over three data points taken from the same substrate at different points.

The atomic force microscopy (AFM) observations of the modified silicon surfaces were carried out with the commercial instrument (Digital Instrument, Nanoscope IIIa, Multimode). All the tapping mode images were taken at room temperature in air with the microfabricated rectangle crystal silicon cantilevers (nanosensor). The topography images were obtained at a resonance frequency of approximate 365 kHz for the probe oscillation.

Fluorescence images were taken at room temperature with a Zeiss Axio Imager A2m Microscope (Carl Zeiss, Germany), equipped with an epi-fluorescence module.

### 2.5. Bacteria adherence on modified surfaces

Bacteria strains of *E. coli* (8099) and *Staphylococcus aureus* (*S. aureus*, ATCC6538) were used in this study.

The bacteria strains were streaked from a glycerol stock onto a BHI agar plate, grown overnight at 37 °C and subsequently used to inoculate 40 mL pre-warmed BHI (no antibiotics) in 100 mL conical flasks. Pre-cultures were grown to mid-exponential phase at 37 °C in a shaking water bath at 250 rpm for 3 h and used to inoculate 40 mL pre-warmed BHI (same batch as pre-culture, no antibiotics) in 100 mL test flasks to a starting OD600 of 0.1 (Corning 259 spectrophotometer).

1 mL samples of this culture was put on the surfaces of interest, and incubated stationary at 37 °C for 2 h. Then the cultured surfaces were washed twice with PBS to remove any loose or unattached bacteria, and stained with fluorescent redox dye DAPI for 1 min. Then washed with PBS and distilled water intensively.

Samples were visualized with a Zeiss Axio Imager A2m Microscope, equipped with an epi-fluorescence module.

## 3. Results and discussion

### 3.1. Preparation and characterization of polymer brushes

The general procedure for preparation of polymer brushes on silicon surface via SI-ATRP is illustrated in Scheme 1. Firstly, a homogeneous monolayer of initiator was immobilized on the silicon surface. Then SI-ATRP was conducted by immersing the initiator modified silicon wafers into the reaction mixture.

For initiator preparation, a two-step process was applied. Clean Si surface was firstly treated with dilute HF to form Si—H surface, then UV-induced hydrosilylation of undecenol with the Si—H surface was used, allowing the formation of robust Si—C linkages [31]. The hydroxyl (—OH) group of the tethered undecenol was then reacted with BIBB and surface ATRP initiator was formed. SI-ATRP was proceeded with OEGMA/PPMA/CuBr/PMDETA molar feed ratio of 60:40:1:1 in a 4:1 mixture of methanol and water at 40 °C. The polymerization was conducted for 12 h, after which the thickness did not increase anymore according to our monitor on the time-dependent thickness change. Alkynyl groups of PPMAs provided the pendants for further immobilization and OEGMA was used for adjusting the pendant density. From ellipsometry, the dry thickness of the monolayer before SI-ATRP was 46.1 ± 2.3 Å, while after 12 h polymerization, the brushes gave a thickness of 268.0 ± 9.1 Å (Table 1).

XPS is widely used in surface information analysis [17,32]. Selected XPS spectra of films at different stages are presented in Fig. 1. For the initiator layer (Fig. 1a), there were evident O, C, Si and Br signals. The narrow scan of Br 3d region (Fig. 1d) showed an emission at 73.5 eV, assigned to the Br atom decorated at the end of

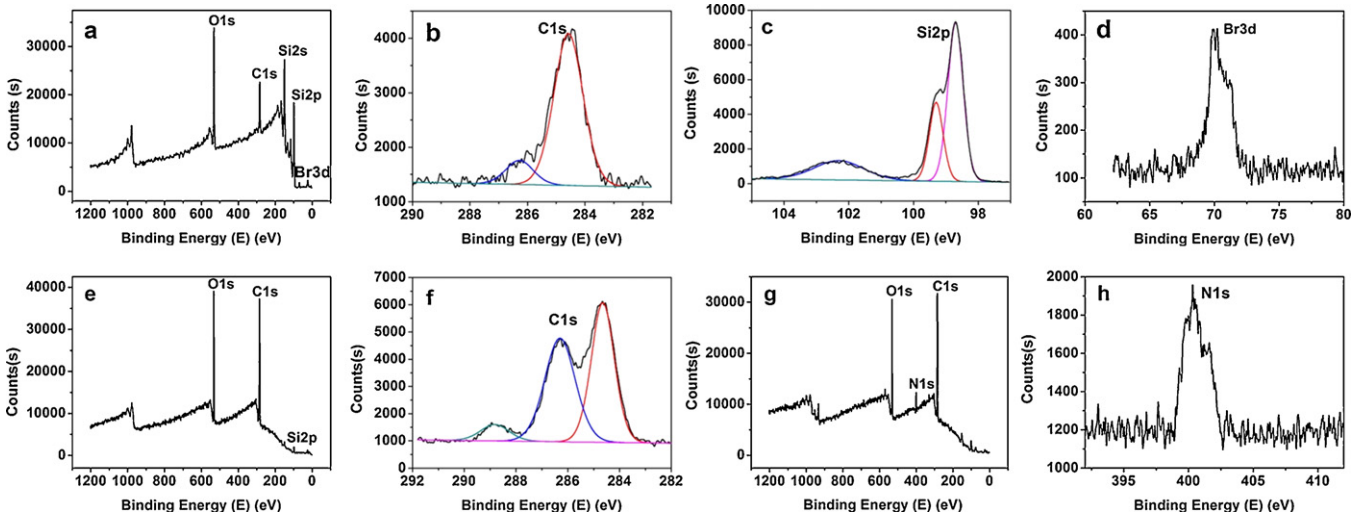


**Fig. 1.** Selected XPS data obtained during several stages of surface functionalization. Panel (a) is the survey scan of the initiator layer and Panels (b)–(d) are the narrow scans for C 1s, Si 2p, Br 3d. Panel (e) is the survey scan of surface after SI-ATRP and Panel (f) is the corresponding narrow scans for C 1s. Panel (g) is the survey scan after CuAAC reaction with mannose and Panel (h) is the corresponding narrow scan for N 1s.

the initiator layer. The Si 2p showed strong emission at 98.5 eV and 99.5 eV (Fig. 1c), which attributed to the Si atoms linked to C and H. There was also a small emission at 102.2 eV, which belonged to Si oxidized by oxygen left in the system. The C 1s region (Fig. 1b) displayed two deconvoluted signals at 284.6 and 286.5 eV, assigned to mostly of C—H and a small portion of C—O respectively. After SI-ATRP, there were clear changes of the survey scan. As shown in Fig. 1e, there were evident C and O signals and the Si signal became quite small, which confirmed that polymer brushes covered the whole surface uniformly. Great differences can also been seen from the C 1s spectrum before (Fig. 1b) and after (Fig. 1f) polymerization. The emission at 285.8 eV (C—O) became quite strong and evident C=O signal (288.5 eV) appeared. These are clear reflections of surface composition changes.

The static contact angle measurement at room temperature indicates variations of wettability of the functionalized silicon surface at different steps. As listed in Table 1, for Si-undecenol layer, the contact angle was $75.2 \pm 0.6^{\circ}$. After reaction with BiBB, it became more hydrophobic ($84.5 \pm 1.1^{\circ}$). Then it came back to hydrophilic of $58.8 \pm 0.5^{\circ}$ due to surface copolymerization of OEGMA and PPMA. It was a little higher than that of POEGMA brushes reported in literature [17]. This may be attributed to the more hydrophobic PPMA component in the copolymer. Surface morphologies before and after polymerization were investigated by atomic force microscopy (AFM). Height images were shown in Fig. 2. For the initiator layer, the surface was quite smooth with a root-mean-square (rms) roughness of 0.109 nm (Fig. 2a), while the polymer brushes modified surface appeared rougher and the corresponding root-mean-square (rms) roughness became 0.634 nm (Fig. 2b). These all indicate the successful construction of the copolymer brushes on silicon wafers.

### 3.2. Functionalization of the brushes using CuAAC reaction

For post-modification of the surface, efficient reaction for coupling biomolecules to the polymer brushes is essential. Herein, CuAAC reaction was applied due to its high efficiency and widely use in biological systems. After copolymerization of the two monomers, the "clickable" polymer brushes were functionalized by "click" reaction of different azido molecules to the alkyne pendants. In addition, microwave was used to accelerate the click reaction rate.

In order to investigate whether azido molecules could be attached to the brushes through the 1,3-dipolar cycloaddition process, a fluorescent 1,3-dipolar cycloaddition reaction was tested on the surface. The 3-azidocoumarins dyes (***1***, Scheme 1) show no fluorescence due to the quenching effect from the electron-rich R-nitrogen of the azido group at the 7-position [33,34]. While after "click" reaction, the fluorescent signals will be "triggered on" for the formation of triazole rings. This could be viewed as a probe for the reaction process on the surfaces. The reaction was proceeded in water/ethanol/DMF (5:2:3) solvent with CuBr as the catalyst. The

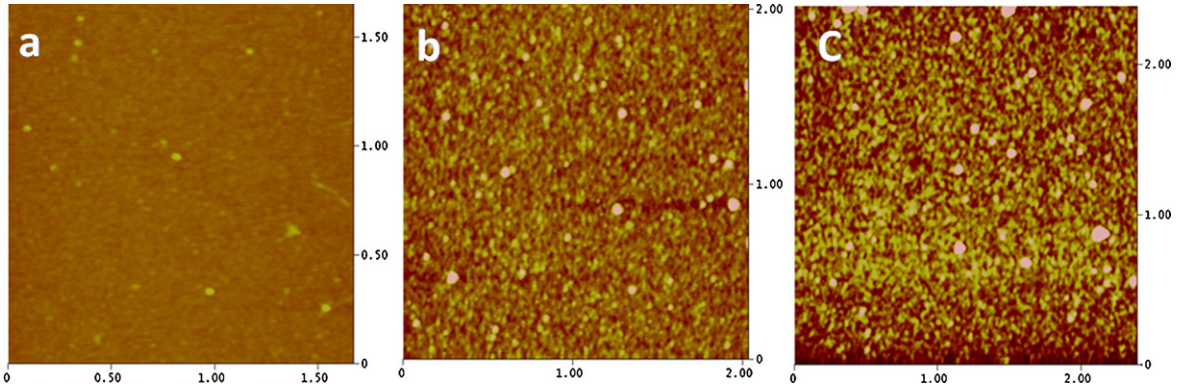


**Fig. 2.** AFM topographic images of silicon surface at different stages: (a) Si-initiator layer, (b) polymer brushes formed after SI-ATRP, and (c) after "click" with mannose.

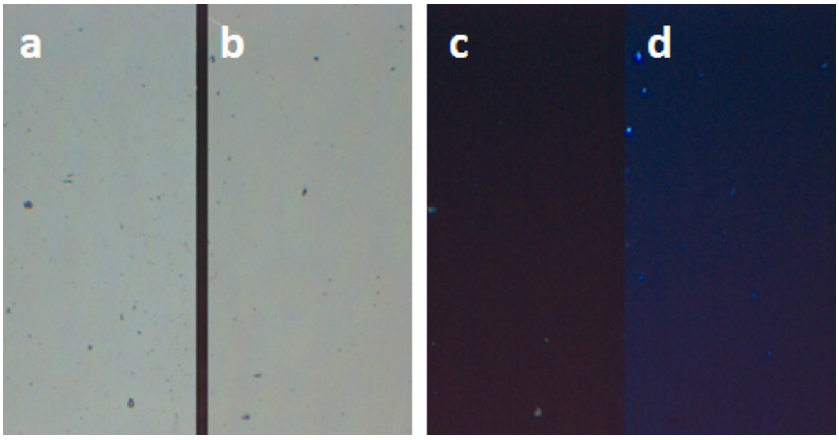


**Fig. 3.** Images of silicon surfaces before (a and c) and after (b and d) "click" with 3-azidocoumarins. (a and b) Bright mode; (c and d) fluorescent mode.

results were shown in Fig. 3 and silicon wafer that did not react with azidocoumarin was set as a comparison. Under bright mode, there was no difference between the two wafers. While under fluorescent mode, the wafer coupled with coumarin showed clear fluorescence. This proved that azido molecules could be coupled to the nanobrushes through CuAAC reaction.

Next, the synthesized azido molecules (***2***, ***3***, ***4***, Scheme 1) were used for surface modification. ***3*** and ***4*** are both monosaccharide and were used for surface glycosylation and ***2*** was used as control. The reaction was carried out under the same conditions as described before. Similarly, XPS was used to characterize the surface information after CuAAC reaction. The XPS survey scans of the mannose functionalized surface are shown in Fig. 1g. Evident N 1s signal (400.3 eV, Fig. 1h) appeared due to the introduction of triazole rings. AFM and ellipsometry results showed that the surface morphology (Fig. 2c) and dry thickness (Table 1) did not have evident change after "click" reaction, while the contact angle measurement showed the surface became more hydrophilic ($45.2 \pm 1.4^\circ$, $37.2 \pm 1.1^\circ$ and $35.5 \pm 0.8^\circ$ for ***2***, ***3***, ***4*** respectively, Table 1). These results confirmed successful immobilization of these biomolecules onto the surfaces.

XPS analysis can also provide the element quantitative information, which provides a way for surface quantitative analysis. Although this method may have a random uncertainty between 15% and 20%, it provides a practical surface analysis method and is widely used in literature [15,32].

For the functionalized polymer brushes tethered on the silicon surface, if all the alkynyl groups were coupled with molecules by CuAAC reaction, the theoretic N content was estimated according to Eq. (1), a calculating method also adopted in similar work [15]:

$$N\% = \frac{(1-x) \times n_{\mathrm{N}}}{x \times n_{\mathrm{OEGMA}} + (1-x) \times n_{\mathrm{click}}} \quad (1)$$

$x$ is the fraction of the OEGMA monomer in the copolymer brush. It was assumed to be the same as that of the feed ratio ($x = 0.6$ in this work) based on the mechanism study of copolymerization in solution by ATRP which showed almost same reaction ratios of the

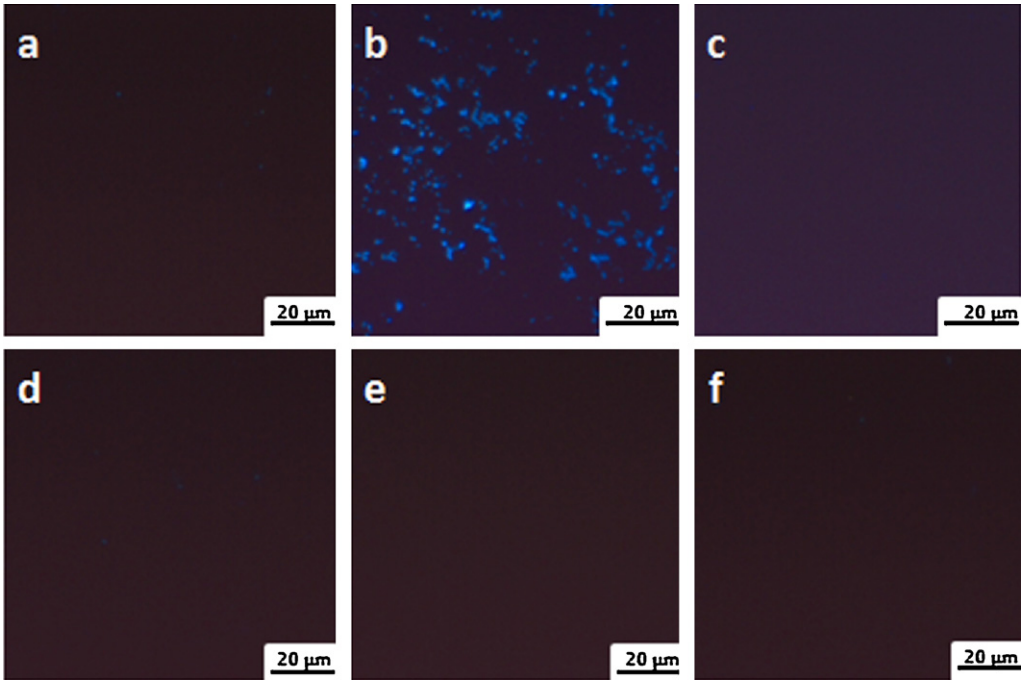


**Fig. 4.** Fluorescent images of various modified surfaces incubated with *E. coli* and *S. aureus*. Panels (a)–(c) were Si surfaces functionalized with (tri) ethylene glycol, mannose and galactose, cultured with *E. coli*. While (d)–(f) were corresponding surfaces cultured with *S. aureus*. Samples were treated with the method described in Section 2.5.

two monomers. $n_N$ is the number of N atoms in the PPMA monomer after CuAAC reaction ($n_N = 3$). $n_{OEGMA}$ is the total number of the atoms in OEGMA monomer ($n_{OEGMA} = 31$), and $n_{click}$ is the number of atoms in PPMA after CuAAC reaction (22 for ***2*** and 26 for ***3***, ***4***).

The theoretic N content of the three reactions are listed in Table 1. Then the "click" efficiency $e$ was obtained as the ratio of the measured N content by XPS over the calculated N content. As listed in Table 1, the click efficiency of ***2***, ***3***, ***4*** were 86%, 61% and 49% respectively. The differences may be attributed to the reactivity, molecule volume and steric hindrance. Mannose and galactose have higher steric hindrance, so the "click" efficiency is relatively lower than (tri) ethylene glycol.

Eq. (2) is always used for calculating the graft density of polymer brushes on surfaces [14,25,35]:

$$\sigma = \frac{h \cdot \rho \cdot N_A}{M_n} \quad (2)$$

$\sigma$ is the graft density (chains $nm^{-2}$) of polymer brushes. $h$ is the dry layer thickness of the polymer brushes used before "click" immobilization, which is determined by ellipsometry. $\rho$ is the bulk density of the polymer layer. $N_A$ is Avogadro's number, and $M_n$ is the number average molecular weight of the polymer chains on the surface.

The surface density of the immobilized molecules can be calculated according to the following equation (3):

$$d = \frac{\sigma \cdot DP \cdot (1 - x) \cdot e}{N_A} \quad (3)$$

$DP$ is the average degree of polymerization ($DP = M_n/(xM_{OEGMA} + (1-x)M_{PPMA})$), and $M_{OEGMA}$, $M_{PPMA}$ represent the molecular weight of OEGMA and PPMA monomer respectively). By combination of Eqs. (2) and (3), the following equation is got:

$$d = \frac{h \cdot \rho \cdot (1 - x) \cdot e}{x \cdot M_{OEGMA} + (1 - x)M_{PPMA}} \quad (4)$$

According to Eq. (4), the surface density is mainly determined by graft thickness and "click" efficiencies of different molecules. This is acceptable because the CuAAC reactions are based on the same polymer brushes and higher surface density can be achieved by producing thicker brushes. For the condition carried out in this work, the dry layer thickness $h$ is 22 nm, and the bulk density $\rho$ is assumed to be 1.2 g/cm$^3$ (1–1.2 g/cm$^3$ was commonly used for polymer brush densities [25,36]). Surface density results calculated from Eq. (4) are listed in Table 1. For the two kinds of monosaccharide used, a quite high surface density of about 4 nmol/cm$^2$ was got. This is quite meaningful for mimicking biosurfaces since "cluster effect" is in widely existence in biological systems.

### 3.3. Surface interaction with bacteria

To evaluate the functionality of biomolecules immobilized on the thin surface films, we investigated the interaction between these modified silicon wafers and two kinds of bacteria. *E. coli* is the most common initiator of urinary tract infections, and possesses rod-like filamentous organelles that protrude from the outer membrane of the cell body. The adhesion FimH proteins on the fimbriae bind specifically to mannose [37]. In addition, this interaction is resistant to fluid flow since FimH can form force-activated catch bonds with mannose [38]. *S. aureus* is a kind of gram-positive coccus. It has no flagellum and no mannose-binding type-1 fimbriae at the surface and is chosen as the negative control.

Three kinds of surfaces were used in this experiment. The mannose-presenting films (Fig. 4b and e) were incubated for 2 h in PBS buffer containing either *E. coli* or *S. aureus*. As controls, films presenting (tri) ethylene glycol (Fig. 4a and d) and galactose (Fig. 4c and f) were likewise exposed to these organisms under identical conditions. After wag and intensive flush, *E. coli* were only left on the mannose-presenting surface while very few left on the (tri) ethylene glycol or galactose presenting surfaces (Fig. 4a–c). The *S. aureus* strain was observed on none of the surfaces after intensively flush and all the surfaces were almost blank (Fig. 4d–f). These results showed that the surfaces decorated with biomolecules maintained their functionalities and can be used as a platform for simulating various functions of surface carbohydrates and investigating carbohydrate-based biological processes.

## 4. Conclusion

In summary, a facile and highly efficient method for surface glycosylation was provided in this article. Silicon surface was firstly covered with copolymer of OEGMA and PPMA via SI-ATRP, followed by microwave assisted CuAAC reaction to immobilize biomolecules onto the alkyne pendants. Based on XPS quantitative analysis, a quite high "click" efficiency and surface glycosyl density was got. It was also shown that upon attaching saccharides onto the thin surface films, the resultant carbohydrate-presenting surfaces maintained their functionalities and showed specific interaction with corresponding binding receptors. We expect that the glycosylation surface can be used as a platform for investigation of interactions between pathogens and surface carbohydrates and the method reported here can be applied for facile and versatile construction of a wide range of functional biosurfaces.

## Acknowledgments

We are grateful for the financial support from the National Natural Science Foundation of China (20974109, 20904053, 50973107, 50973108, 50873102, 50733003), the Knowledge Innovation Program of the Chinese Academy of Sciences (KJCX2-YW-H19), and the Program of Scientific Development of Jilin Province (20090135).

## References

[1] S.L. Flitsch, R.V. Ulijn, Nature 421 (2003) 219–220.
[2] H. Ise, S. Kobayashi, M. Goto, T. Sato, M. Kawakubo, M. Takahashi, U. Ikeda, T. Akaike, Glycobiology 20 (2010) 843–864.
[3] P.I. Kitov, J.M. Sadowska, G. Mulvey, G.D. Armstrong, H. Ling, N.S. Pannu, R.J. Read, D.R. Bundle, Nature 403 (2000) 669–672.
[4] Y.C. Lee, R.T. Lee, Acc. Chem. Res. 28 (1995) 321–327.
[5] S.G. Spain, M.I. Gibson, N.R. Cameron, J. Polym. Sci. A: Polym. Chem. 45 (2007) 2059–2072.
[6] C.S. Xiao, C.W. Zhao, P. He, Z.H. Tang, X.S. Chen, X.B. Jing, Macromol. Rapid Commun. 31 (2010) 991–997.
[7] V. Ladmiral, G. Mantovani, G.J. Clarkson, S. Cauet, J.L. Irwin, D.M. Haddleton, J. Am. Chem. Soc. 128 (2006) 4823–4830.
[8] G. Pasparakis, A. Cockayne, C. Alexander, J. Am. Chem. Soc. 129 (2007) 11014–11015.
[9] G. Coullerez, P.H. Seeberger, M. Textor, Macromol. Biosci. 6 (2006) 634–647.
[10] E.H. Song, N.L.B. Pohl, Curr. Opin. Chem. Biol. 13 (2009) 626–632.
[11] J. Jin Yoon, S. Ho Song, D. Sung Lee, T.G.T.G. Park, Biomaterials 25 (2004) 5613–5620.
[12] V. Vazquez-Dorbatt, Z.P. Tolstyka, C.W. Chang, H.D. Maynard, Biomacromolecules 10 (2009) 2207–2212.
[13] X.L. Sun, C.L. Stabler, C.S. Cazalis, E.L. Chaikof, Bioconj. Chem. 17 (2006) 52–57.
[14] R. Iwata, R. Satoh, Y. Iwasaki, K. Akiyoshi, Colloid Surf. B 62 (2008) 288–298.
[15] G.T. Qin, C. Santos, W. Zhang, Y. Li, A. Kumar, U.J. Erasquin, K. Liu, P. Muradov, B.W. Trautner, C.Z. Cai, J. Am. Chem. Soc. 132 (2010) 16432–16441.
[16] K.A. Barth, G. Coullerez, L.M. Nilsson, R. Castelli, P.H. Seeberger, V. Vogel, M. Textor, Adv. Funct. Mater. 18 (2008) 1459–1469.
[17] F.J. Xu, L.Y. Liu, W.T. Yang, E.T. Kang, K.G. Neoh, Biomacromolecules 10 (2009) 1665–1674.
[18] C. Wang, J.A. Wu, Z.K. Xu, Macromol. Rapid Commun. 31 (2010) 1078–1082.
[19] X. Laloyaux, E. Fautre, T. Blin, V. Purohit, J. Leprince, T. Jouenne, A.M. Jonas, K. Glinel, Adv. Mater. 22 (2010) 5024–5028.
[20] R. Barbey, L. Lavanant, D. Paripovic, N. Schuwer, C. Sugnaux, S. Tugulu, H.A. Klok, Chem. Rev. 109 (2009) 5437–5527.
[21] P.L. Golas, N.V. Tsarevsky, B.S. Sumerlin, K. Matyjaszewski, Macromolecules 39 (2006) 6451–6457.

[22] C.J. Fristrup, K. Jankova, S. Hvilsted, Soft. Matter 5 (2009) 4623–4634.
[23] R. Barbey, E. Kauffmann, M. Ehrat, H.A. Klok, Biomacromolecules 11 (2010) 3467–3479.
[24] M. Ejaz, K. Ohno, Y. Tsujii, T. Fukuda, Macromolecules 33 (2000) 2870–2874.
[25] K. Yu, J.N. Kizhakkedathu, Biomacromolecules 11 (2010) 3073–3085.
[26] H.C. Kolb, M.G. Finn, K.B. Sharpless, Angew. Chem. Int. Ed. 40 (2001) 2004–2021.
[27] J.S. Guo, Y. Wei, D.F. Zhou, P.Q. Cai, X.B. Jing, X.S. Chen, Y.B. Huang, Biomacromolecules 12 (2011) 737–746.
[28] K. Sivakumar, F. Xie, B.M. Cash, S. Long, H.N. Barnhill, Q. Wang, Org. Lett. 6 (2004) 4603–4606.
[29] B.C. Mei, K. Susumu, I.L. Medintz, H. Mattoussi, Nat. Protoc. 4 (2009) 412–423.
[30] J. Geng, G. Mantovani, L. Tao, J. Nicolas, G.J. Chen, R. Wallis, D.A. Mitchell, B.R.G. Johnson, S.D. Evans, D.M. Haddleton, J. Am. Chem. Soc. 129 (2007) 15156–15163.
[31] R.L. Cicero, M.R. Linford, C.E.D. Chidsey, Langmuir 16 (2000) 5688–5695.
[32] D.Y. Petrovykh, H. Kimura-Suda, M.J. Tarlov, L.J. Whitman, Langmuir 20 (2004) 429–440.
[33] M.S. Schiedel, C.A. Briehn, P. Bauerle, Angew. Chem. Int. Ed. 40 (2001) 4677–4680.
[34] D.J. Yee, V. Balsanek, D. Sames, J. Am. Chem. Soc. 126 (2004) 2282–2283.
[35] Q. Yu, Y.X. Zhang, H. Chen, Z.Q. Wu, H. Huang, C. Cheng, Colloid Surf. B 76 (2010) 468–474.
[36] X. Laloyaux, B. Mathy, B. Nysten, A.M. Jonas, Langmuir 26 (2010) 838–847.
[37] P. Aprikian, V. Tchesnokova, B. Kidd, O. Yakovenko, V. Yarov-Yarovoy, E. Trinchina, V. Vogel, W. Thomas, E. Sokurenko, J. Biol. Chem. 282 (2007) 23437–23446.
[38] W.E. Thomas, E. Trintchina, M. Forero, V. Vogel, E.V. Sokurenko, Cell 109 (2002) 913–923.